Abnormal Lateral Geniculate Nucleus and Optic Chiasm in Human Albinism

Larissa Mcketton,[1,2] Krista R. Kelly,[2,3] and Keith A. Schneider[1,2]*

[1]Department of Biology, York University, Toronto, Ontario, Canada
[2]Centre for Vision Research, York University, Toronto, Ontario, Canada
[3]Department of Psychology, York University, Toronto, Ontario, Canada

ABSTRACT

Our objective was to measure how the misrouting of retinal ganglion cell (RGC) fibers affects the organization of the optic chiasm and lateral geniculate nuclei (LGN) in human albinism. We compared the chiasmal structures and the LGN in both pigmented controls and patients with albinism by using high-resolution structural magnetic resonance imaging (MRI). We studied 12 patients with oculocutaneous albinism and 12 age-matched pigmented controls. Using a 3T MRI scanner, we acquired a T_1-weighted three-dimensional magnetization-prepared rapid gradient-echo (MPRAGE) image of the whole brain, oriented so that the optic nerves, chiasm, and tracts were in the same plane. We acquired multiple proton density-weighted images centered on the thalamus and midbrain, and averaged them to increase the signal, enabling precise manual tracing of the anatomical boundaries of the LGN. Albinism patients exhibited significantly smaller diameters of the optic nerves, chiasm and tracts, and optic chiasm and LGN volume compared with controls ($P < 0.001$ for all). The reductions in chiasmal diameters in the albinism compared with the control group can be attributed to the abnormal crossing of optic fibers and the reduction of RGCs in the central retina. The volume of the LGN devoted to the center of the visual field may be reduced in albinism due to fewer RGCs representing the area where the fovea would normally lie. Our data may be clinically useful in addressing how genetic deficits compromise proper structural and functional development in the brain. J. Comp. Neurol. 522:2680–2687, 2014.

INDEXING TERMS: albinism; lateral geniculate nucleus; optic chaism; magnetic resonance imaging

Albinism, a genetic condition of hypopigmentation, is caused by melanocyte or melanin depletion (Kugelman and Van Scott, 1961). Melanin plays a significant role during typical ocular development. If melanin is absent, the fovea fails to develop properly, and neural connections between the retina and brain are altered (Fulton et al., 1978). As a result, those with albinism display a variety of ophthalmic deficits including reduced visual acuity (Fonda et al., 1971) and nystagmus (Rosenberg and Jabbari, 1987; Summers, 1996). In the human visual pathway, approximately half of retinal ganglion cell (RGC) axons cross at the chiasm (i.e., nasal retinal fibers), whereas the other half project ipsilaterally (i.e., temporal retinal fibers) to both lateral geniculate nuclei (LGN). The LGN is the primary subcortical visual relay nucleus (Kastner et al., 2006) and is organized into six interleaved monocular layers: the dorsal four parvocellular (P) layers and the dorsal two magnocellular (M) layers. In the albinism visual pathway, a large proportion of RGC axons from the temporal retina are misrouted and cross at the optic chiasm, as seen in mammals such as cats (Creel, 1971), rats (Lund, 1965), tigers (Guillery and Kaas, 1973), and humans (Carroll et al., 1980; Creel et al., 1974, 1978; Hoffmann et al., 2005; Morland et al., 2002; von dem Hagen et al., 2008). For example, in human albinism there is an increase in crossing over of 70–85% of retinal fibers at the optic chiasm, whereas 15–30% of fibers project ipsilaterally. This misrouting leads to an abnormal arrangement of fibers projecting to the LGN, with a

Grant sponsor: The Dana Foundation; Grant sponsor: the Natural Sciences and Engineering Research Council of Canada (NSERC).

*CORRESPONDENCE TO: Keith Schneider, Sherman Health Science Research Centre, 4700 Keele Street, Toronto, ON M3J 1P3, Canada. E-mail: keiths@yorku.ca

Received December 20, 2013; Revised February 16, 2014;
Accepted February 18, 2014.
DOI 10.1002/cne.23565
Published online April 12, 2014 in Wiley Online Library (wileyonlinelibrary.com)

TABLE 1.
Albinism participant characteristics

Patient	Age (yr)	Sex	Albinism classification	Visual acuity	Optical correction					
					Sphere		Cylinder		Axis	
					OD	OS	OD	OS	OD	OS
A1	48	M	OCA	0.6	+7.75	+8.00	−5.75	−5.00	010	163
A2	46	F	OCA-1	0.7	+5.50	+5.00	−3.25	−2.50	004	177
A3	19	M	OCA-1	0.8	+11.5	+10.7	−3.00	−2.75	–	–
A4	21	M	OCA-1a	1.0	No corrective lenses					
A5	48	M	OCA-1	1.0	−4.00	−2.25	−0.50	−2.25	016	150
A6	44	F	OCA-1	0.8	+7.00	+6.25	−3.25	−2.50	175	180
A7	56	M	OCA	0.9	+2.25	+2.25	−2.50	−1.75	009	163
A8	22	F	OCA	0.6	+2.50	+4.50	−2.75	−4.25	017	166
A9	47	F	OCA	0.9	+1.00	+2.00	–	–	–	–
A10	45	F	OCA	1.0	+10.0	+10.0	–	–	–	–
A11	17	F	OCA-1	0.9	+5.50	+5.75	−3.50	−3.50	005	180
A12	29	F	OCA-2	0.5	−12.50	−12.25	−3.00	−3.00	010	169

Visual acuity was measured with the ETDRS LogMAR eye chart. Also included are the prescriptions of those who wore corrective lenses.
Abbreviations: OCA, oculocutaneous albinism; OCA1, tyrosinase-related oculocutaneous albinism with no functional tyrosinase (OCA1a); OCA2, with functional tyrosinase enzyme.

predominant representation of just one eye in the contralateral hemisphere (Guillery et al., 1975). In animal models of albinism, cats (Guillery et al., 1974), minks (Sanderson et al., 1974), and monkeys (Guillery et al., 1984) exhibit fusion of LGN layers.

Relatively little research has been conducted on the development of the LGN in humans with albinism. One postmortem study compared LGN morphology of a single human with albinism with a visually intact control (Guillery et al., 1975). The albinism subject displayed fusions among the M and P layers, as would be expected when neighboring layers receive a larger proportion of the crossing nasal fibers. These layers would then be innervated by the same eye, and in a sense be monocular. The LGN of the albinism subject appeared to be smaller, and abnormal in shape and orientation, displaying an elevated lateral tip (Guillery, 1986; von dem Hagen et al., 2008). However, this has been the only study to examine the LGN in human albinism (Guillery et al., 1975). Moreover, only one participant with albinism was compared with one control, and this was conducted post mortem. It is unclear whether these proportions are general properties of the LGN in albinism or due to extensive individual variability of the LGN (Hickey and Guillery, 1979). In the present study, we investigated the consequences of fiber misrouting on the development of the LGN in living human participants with albinism.

Our primary focus was to compare LGN volume between pigmented controls and participants with albinism using high-resolution structural magnetic resonance imaging (MRI). Prior studies have described the visibility of the LGN using proton density-weighted (PD) MRI scans (Bridge et al., 2008; Fujita et al., 2001; Gupta et al., 2009) that were able to differentiate thalamic nuclei in controls (Devlin et al., 2006). By acquiring multiple PD-weighted images, we were able to precisely determine the anatomical boundaries of the human LGN and obtain an accurate measure of its volume. Based on a smaller LGN in a postmortem albinism subject (Guillery et al., 1975), we predict smaller LGN volumes in the albinism group compared with controls. Due to previous inconsistencies, our secondary focus was to confirm previously found decreases in optic nerve, chiasm, and tract measurements in human albinism. To accomplish this, we used a 3T MRI scanner with 1-mm^3 isotropic voxel size to obtain higher resolution images than those previously reported. This research was conducted to add to the body of knowledge about the development and plasticity of the LGN in the human thalamus.

MATERIALS AND METHODS

Participants

Twelve patients with oculocutaneous albinism (OCA) with a mean age ± standard error of the mean (SEM) of 37 ± 4 years (seven female) were compared with 12 age-matched controls, 32 ± 3 years (six female). All participants were in good health with no history of neurological disorders. Visual acuity measurements were performed by using an ETDRS LogMar eye chart (Precision Vision, La Salle, IL) on all participants. Table 1 includes albinism patient history and optical correction. All controls had normal or corrected-to-normal visual acuity (20/20) or better. All participants gave written informed consent, and the experimental protocol was approved by the York University Human Participants Review Committee.

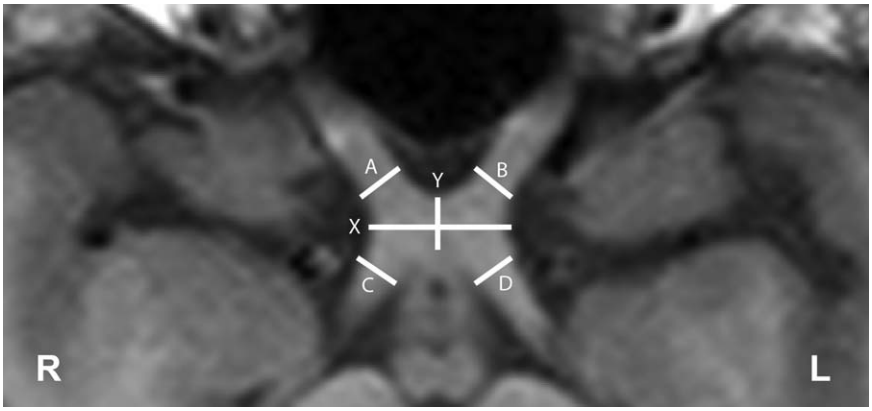

Figure 1. Axial image of a T_1-weighted scan from a control participant displaying the (A) right and (B) left optic nerves, optic chiasm widths in the mediolateral (X) and anteroposterior (Y) dimensions, and the (C) right and (D) left optic tracts.

Optic chiasm measurements

Participants were scanned by using a Siemens (Erlangen, Germany) Trio 3T MRI scanner and 32-channel head coil in the Neuroimaging Laboratory at the Sherman Health Sciences Research Centre at York University. To reduce head motion, cushions were placed around the participants' heads. A T_1-weighted three-dimensional magnetization-prepared rapid gradient-echo (MPRAGE) image of the entire head with a 1-mm^3 isotropic voxels was acquired with the following parameters: TR = 1.9 s, TE = 2.52 ms, 1-mm slice thickness, 256 × 256 matrix, 9° flip angle, parallel imaging acceleration factor (generalized autocalibrating partially parallel acquisition [GRAPPA]) = 2. For all T_1-weighted images, the optic nerves, optic chiasm, and optic tracts were reoriented in the same plane, resulting in a reformatted image that was parallel to the optic chiasm. Three independent raters blind to group membership manually traced the optic chiasm region-of-interest (ROI) using FSLView software (v. 4.1.8, http://www.fmrib.ox.ac.uk/fsl). The volume of the optic chiasm was measured on the median of these three masks for each participant. Measurements of the right and left optic nerves, right and left optic tracts, and optic chiasm widths in the mediolateral and anteroposterior planes were also performed three times each by four raters who were blind to group membership using the OsiriX length measurement tool (Rosset et al., 2004) (Fig. 1).

LGN volume

A series of 30–40 PD-weighted images were acquired coronally with 19–48 slices, 1 or 2 mm thick, 256 × 256 matrix, 192-mm field of view, 0.75 × 0.75 mm^2 in-plane resolution, TR = 3 s, TE = 26 ms, flip angle = 120°, and parallel imaging acceleration factor (GRAPPA) = 2. Each volume acquisition took 89 s. The PD-weighted scans were interpolated to twice the resolution in each dimension, registered, corrected for motion between acquisitions using the flirt program from the FSL software package, and averaged. Three independent raters blind to group membership manually outlined the anatomical boundaries of the LGN three times each. The resulting ROIs were merged, creating a median mask for each rater, and the median of these was used to measure LGN volume (Fig. 2). All statistics were computed with SPSS Version 20 for Mac (IBM, Armonk, NY).

Whole brain volume

Whole brain volumes were calculated from each participant by using volumetric segmentation that excluded the cerebellum and brainstem using Freesurfer software (http://surfer.nmr.mgh.harvard.edu).

RESULTS

Intra- and inter-rater reliability

Intraclass correlation coefficient (ICC) reliability analyses were conducted to ensure consistent measurements within (intra) and between (inter) raters. For chiasm measurements, all intra-rater ICCs were above 0.74, and all inter-rater ICCs were above 0.91. For LGN volume, all intra-rater ICCs were above 0.93, and all inter-rater ICCs were above 0.89. ICCs above 0.70 are considered to reflect a reliable measure (Cohen, 2001); thus our ICCs indicate that measurements were consistent both within and between raters.

Whole brain volume

The whole brain volume was (mean ± SEM) 1,097 ± 25 cm^3 for the control group and 1,027 ± 29 cm^3 for the albinism group (Table 2). These volumes were in the same range as previously reported for healthy controls (Allen et al., 2002). No significant group difference in whole brain volume was found, $t(22) = -1.81$, $P = 0.084$.

Optic nerve and optic tract diameter

The respective mean diameters for the right and left optic nerves were 4.81 ± 0.18 mm and 4.78 ± 0.15 mm for the control group, and 3.81 ± 0.01 mm and 3.77 ± 0.08 mm for the albinism group. The respective mean diameters for the right and left optic tracts were 4.28 ± 0.14 mm and 4.23 ± 0.12 mm for the control

group, and 3.29 ± 0.08 mm and 3.40 ± 0.09 mm for the albinism group.

A 2 × 2 × 2 mixed model analysis of covariance (ANCOVA) with group (albinism and control) as the between-group variable, hemisphere (left and right) and diameter (optic nerve and optic tract) as the within-subject variables, and brain volume and age as covariates revealed no significant group by hemisphere interaction, $F(1,20) = 0.90$, $P = 0.35$, or group by diameter interaction, $F(1,20) = 0.25$, $P = 0.62$. However, there was a significant main effect of group, $F(1, 20) = 39.0$, $P < 0.001$.

Post hoc pairwise comparisons (Bonferroni-adjusted $\alpha = 0.013$) revealed that the albinism group had significantly decreased left and right optic nerve and optic tract diameters compared with the control group ($P < 0.001$ for all) (Fig. 3).

Optic chiasm width and volume

The optic chiasm width in the mediolateral plane was 13.01 ± 0.35 mm in the control group and 9.65 ± 0.31 mm in the albinism group. Chiasm width in the anteroposterior plane was 4.37 ± 0.22 mm in the control group and 4.01 ± 0.12 mm in the albinism group. Chiasm volume was 367 ± 15 mm^3 in the control group and 252 ± 12 mm^3 in the albinism group.

A 2 × 3 mixed model ANCOVA, with group (albinism and control) as the between-group variable, chiasm measurements (mediolateral width, anteroposterior width, and chiasm volume) as the within-subject variables, and brain volume and age as covariates revealed a significant group by chiasm measurement interaction, $F(2,40) = 35.4$, $P < 0.001$, and a significant main effect of group, $F(1,20) = 35.6$, $P < 0.001$.

Post hoc pairwise comparisons (Bonferroni-adjusted $\alpha = 0.017$) revealed that the albinism group had significantly decreased chiasm volume and chiasm width in the mediolateral plane ($P < 0.001$), but not in the anteroposterior plane ($P = 0.10$) (Fig. 4).

LGN volume

The respective right and left mean LGN volumes were 165.2 ± 9.6 mm^3 and 157.9 ± 9.8 mm^3 for the control group, and 105.6 ± 8.7 mm^3 and 98.2 ± 6.0 mm^3 for the albinism group.

A 2 × 2 mixed model ANCOVA with group (albinism and control) as the between-group variable, hemisphere (left and right) as the within-subject variable, and brain volume and age as covariates revealed no significant group by hemisphere interaction, $F(1,20) = 0.11$, $P = 0.75$, and no significant main effect of hemisphere, $F(1, 20) = 0.14$, $P = 0.71$. However, there was a significant main effect of group, $F(1, 20) = 22.1$, $P < 0.001$.

Post hoc pairwise comparisons (Bonferroni-adjusted $\alpha = 0.025$) revealed significantly decreased left ($P < 0.001$) and right ($P = 0.001$) LGN volumes in albinism participants compared

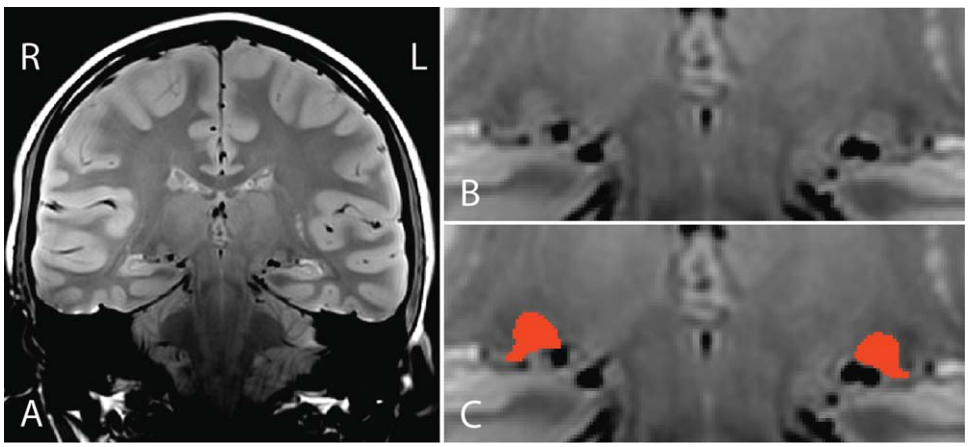

Figure 2. **A**: An example of an averaged coronal PD-weighted image slab that was interpolated to twice the resolution and half the voxel size in a control participant. **B:** Zoomed-in view of the right and left LGN. **C:** Manually traced right and left LGN regions of interest.

TABLE 2.

Descriptive statistics for the control and albinism groups showing the mean (SEM) optic nerve diameter, optic chiasm width in the X and Y planes, optic chiasm volume, optic tract diameter, LGN volume, and whole brain volume.

	Optic nerve diameter (mm)		Optic chiasm width (mm)		Optic chiasm volume (mm^3)	Optic tract diameter (mm)		LGN volume (mm^3)		Whole brain volume (cm^3)
Group	Right	Left	X Plane	Y Plane		Right	Left	Right	Left	
Control	4.8 (0.18)	4.8 (0.15)	13 (0.35)	4.4 (0.22)	364 (14.6)	4.3 (0.14)	4.2 (0.12)	165 (9.6)	158 (9.8)	1,097 (25.2)
Albinism	3.8 (0.01)	3.8 (0.08)	9.7 (0.31)	4 (0.12)	252 (11.5)	3.3 (0.08)	3.4 (0.09)	106 (8.7)	98 (6.0)	1,027 (29.3)
P value	<0.001	<0.001	<0.001	0.103	<0.001	<0.001	<0.001	<0.05	<0.05	0.084

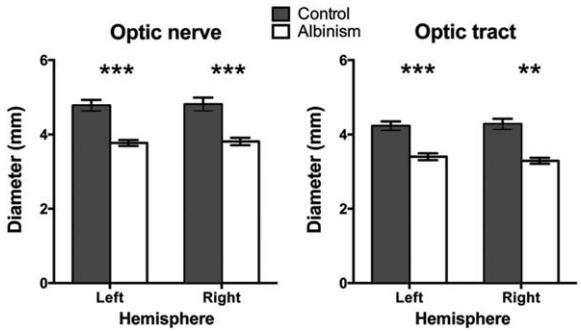

Figure 3. Bar graphs depicting mean optic nerve and optic tract diameters (mm) for the control (dark gray bars) and albinism (white bars) groups. The albinism group exhibited significant decreases in optic nerve and optic tract measures compared with the control group. Error bars represent ±SEM. **, $P < 0.01$; ***, $P < 0.001$.

with controls. There were no significant differences between the left and right LGN volume within albinism ($P = 0.22$) or control ($P = 0.44$) groups (Fig. 5). There were no significant correlations between visual acuity and volume for either the left ($r = 0.11$) or right ($r = 0.33$) LGN, $n = 12$, two-tailed $P > 0.05$ in the albinism group. There was a highly significant positive correlation between the ipsilateral optic tract width and LGN volume as an average across hemispheres in the control and albinism group ($r = 0.53$, $P < 0.01$) (Fig. 6).

DISCUSSION

Here, we report significantly smaller bilateral LGN in the albinism group compared with the control group. In the present study, the LGN volumes in controls ranged from 110.1 to 278.8 mm^3, and compared well with those reported in previous postmortem studies (Allen et al., 2002; Andrews et al., 1997).

The LGN in albinism is abnormal in that layers that are adjacent to one another do not receive the proper overlapping representations of the visual hemifield that originate from the opposite eyes as they normally would (Guillery et al., 1974). This means that visual information is abnormally sent to the visual cortex, resulting in abnormal topographical mapping of the visual field to the cortical surface. Because humans with albinism have approximately the most central 8° of their temporal retina abnormally decussate to the contralateral hemisphere (Hoffmann et al., 2005), this portion of the visual field in the LGN does not encompass the normal contralateral visual field maps represented in both eyes. Instead, the LGN in albinism is comprised of maps of the contralateral and ipsilateral visual fields that are represented by input predominantly from the contralateral eye. As a result, the visual cortex in albinism lacks binocular input and instead receives input from both visual fields (Klemen et al., 2012).

In human albinism, no known documented studies have described the retinotopic organization and volume disparities of the LGN. Normally in the LGN, as in the retina and visual cortex, the central visual

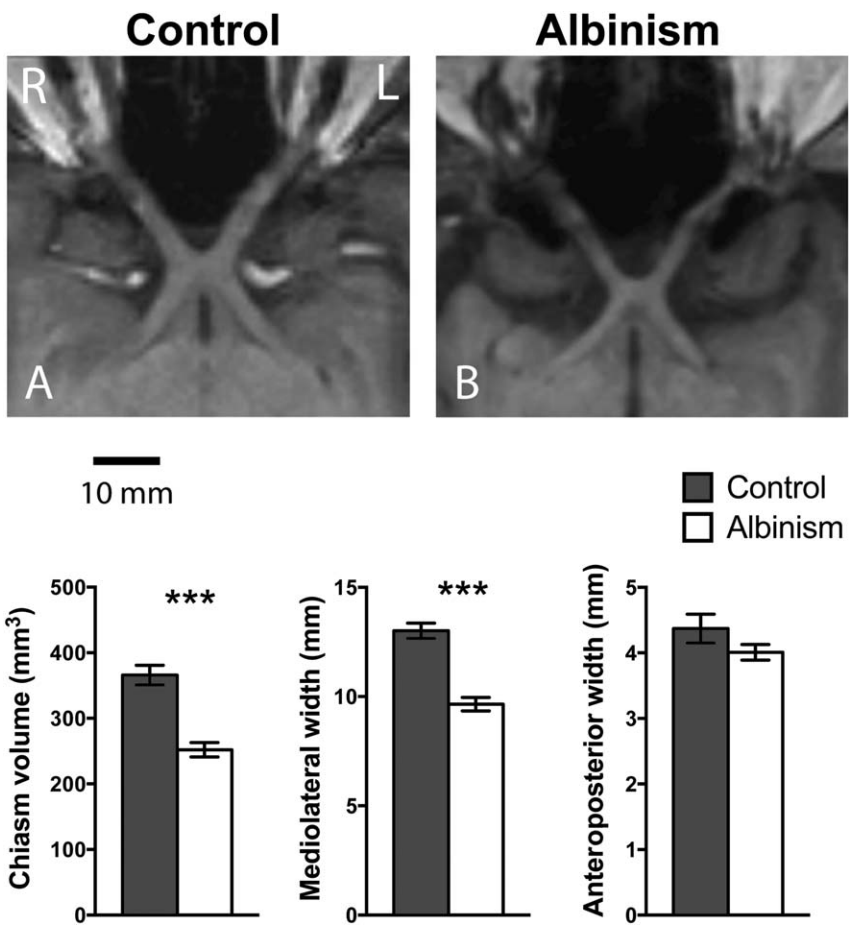

Figure 4. **A,B**: Optic chiasm of a (A) control participant and (B) albinism participant. Bar graphs depicting mean optic chiasm volume and mean optic chiasm width in the mediolateral and anteroposterior dimensions, for the control (dark gray bars) and albinism (white bars) groups. The albinism group exhibited significant decreases in the chiasm volume and mediolateral width but not in the anteroposterior width compared with the control group. Error bars represent ±SEM. ***, $P < 0.001$. Scale bar = 10 mm in A (applies to A,B).

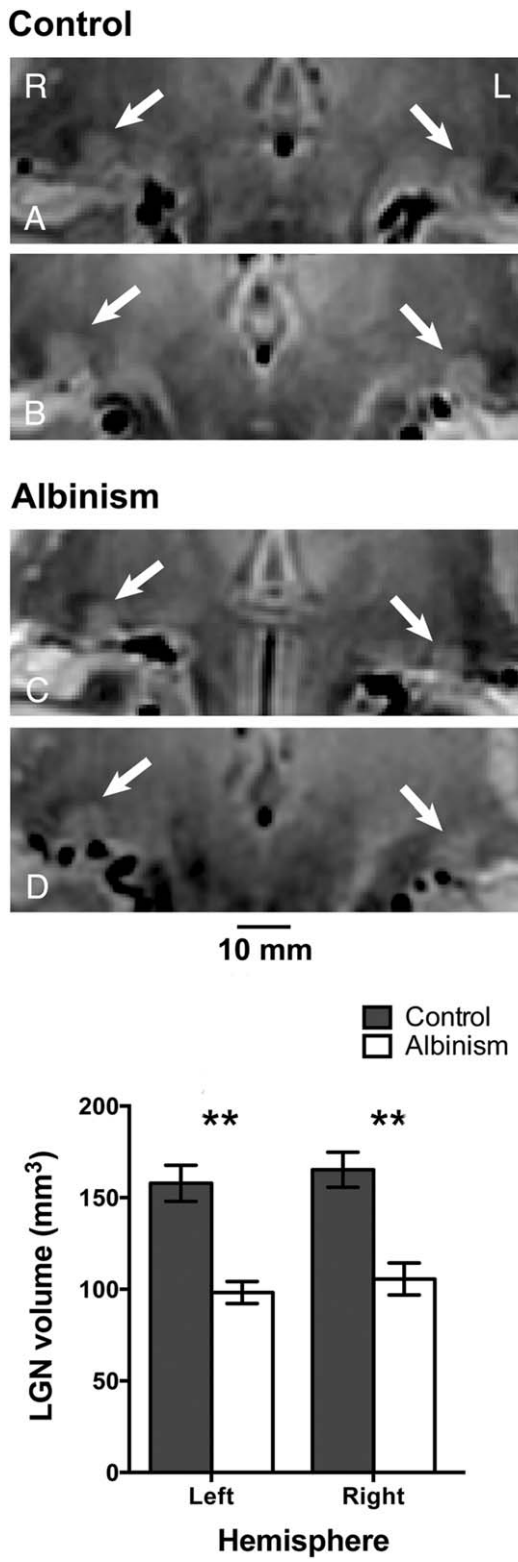

Figure 5. **A–D**: PD-weighted images of the left and right LGN for control participants (A) female 42, (B) male 25, and albinism participants (C) male 48, (D) female, 21. Bar graphs depicting mean volumes of the left and right LGN for the control (dark gray bars), and the albinism (white bars) group. The albinism group showed significant volume decreases in both LGN compared with control group. Error bars represent ±SEM. **, $P < 0.01$. Scale bar = 10 mm in D (applies to A–D).

field is over-represented, with a larger fraction of neurons devoted to its processing compared with more peripheral locations. The fovea is represented in the posterior and superior portions of the LGN, whereas more peripheral representations of the visual field are situated more laterally and anteriorly (Malpeli and Baker, 1975; Schneider et al., 2004). The reduction in the central RGCs and absent fovea in albinism may then cause narrowed optic nerves, chiasm, and tracts. The decrease in these structures likely result in significantly smaller LGN and may therefore result in further downstream decreases in the graymatter cortical volume at the occipital poles that correspond to cortical representations of the central retina (Fujita et al., 2001; von dem Hagen et al., 2005). A recent study that assessed a large population of albinotic subjects found decreased gyrification in the left occipital lobe of the ventral extrastriate cortex (Bridge et al., 2012). This further corroborates that decreases of the foveal regions and their inputs to a decreased LGN volume may then be indicative of decreased graymatter cortical volumes in these regions.

Previous studies examining chiasmal structures in human albinism have yielded inconsistent results. One study found no abnormalities in the optic nerve or optic chiasm (Brodsky et al., 1993); however, this study did not compare albinism participants with a normal pigmented control group. Furthermore, whereas one study found decreases in the optic nerve, optic chiasm, and optic tract diameters of albinism participants compared with controls (Schmitz et al., 2003), another study found decreases in optic nerve and chiasm measures, but no difference in optic tract diameters (von dem Hagen et al., 2005). These discrepancies may be due to differences in MRI acquisition parameters, with the first study having a lower resolution than more recent studies. In addition, the images in the first study were not reformatted in an axial oblique plane parallel to the optic nerves and tracts, and were acquired with an in-plane spatial resolution of 1.2 mm (Brodsky et al., 1993). In contrast, other studies have used either a 1T (Schmitz et al., 2003), or 1.5T (von dem Hagen et al., 2005) MRI scanner and a higher in-plane spatial resolution of 1 mm, whereas our study used a 3T MRI scanner with a higher in-plane spatial resolution of 1 mm.

In the present study, control participants' optic nerve and tract diameters, as well as chiasm measurements, were in the same range as in previous studies (Allen et al., 2002; Guillery, 1986; Parravano et al., 1993; Wagner et al., 1997). Our findings reveal significantly smaller optic chiasm width, optic nerve and optic tract diameters, and optic chiasm volumes in the albinism compared with the control group. These decreases may

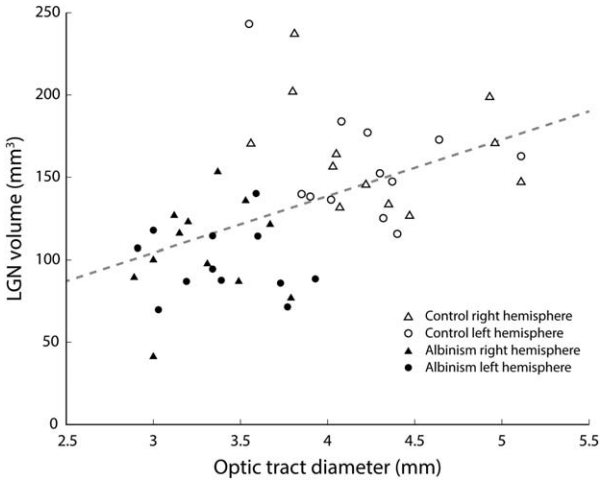

Figure 6. Scatterplot correlation between the ipsilateral optic tract width and LGN volume in both albinism and control groups. Triangles denote the control group, circles denote the albinism group, solid markers denote the right LGN, and open markers denote the left LGN. The dashed line indicates the highly significant correlation between the optic tract diameter and the ipsilateral LGN volume as an average across hemispheres ($P < 0.01$).

be attributed to the reduction of RGCs in the central retina, as found in primates with albinism (Guillery et al., 1984), and an absent fovea, as found in human albinism (Elschnig, 1913).

In a previous study, a decrease in the number of optic nerve fibers between albino and pigmented rats was reported (albino 74,800, pigmented 80,100) (Bruesch and Arey, 1942). However, later studies in albino mice found that the overall population of optic nerve RGCs was not statistically different from their pigmented counterparts (Salinas-Navarro et al., 2009). Although there is a reduction in RGC fibers in the central retina in albinism, it may be the case that more RGC fibers are present in the periphery because the total number of RGC fibers is the same and the width differences would not be attributed to the fiber count alone.

To understand visual system development in humans, we cannot do manipulative experiments, but rather we can examine clinical populations with altered development. The visual pathway in albinism has been studied in nonprimates and primates, revealing a number of abnormalities from the retina to the visual cortex. More studies need to be conducted to determine whether a decrease in LGN volume is related to a decreased number of RGC nerve fibers that innervate the LGN, a collapse of the layers in LGN, or a decrease in each of the layers individually. Future research in delineating the LGN layers with high-resolution MRI will clarify this issue.

In conclusion, we found structurally significant decreases in chiasmal structures and the LGN in the albinism group compared with controls. Morphological differences at the level of the retina and chiasm have continued to be well defined, but here we provide the first study to compare LGN volumes in living human albinism with their pigmented counterparts. A better understanding of the degree of structural changes in the LGN, and the thalamus in general, following atypical visual development may assist in assessing potential improvements in overall visual performance and the effectiveness of certain treatments.

ACKNOWLEDGMENTS

The authors thank the albinism patients for participating in this research study and Dr. Rick Thompson for his assistance in recruiting participants. The authors also thank raters Saadia Malik and Stefania Moro for their help with the chiasm and LGN measurements and tracings. Lastly, the authors acknowledge Joseph Viviano, Kevin DeSimone, and Mónica Giraldo for their knowledge and help in analyzing the LGN data as well as Joy Williams and Aman Goyal for their MRI acquisition and analysis expertise.

CONFLICT OF INTEREST STATEMENT

All authors declare no conflict of interest.

ROLE OF AUTHORS

All authors had full access to all the data in the study, and take responsibility for the integrity of the data and accuracy of the data analysis. LM designed the research, acquired the data, analyzed the data, and wrote the paper. KRK analyzed the data and wrote the paper. KAS designed the research, wrote the paper, and secured the funding.

LITERATURE CITED

Allen JS, Damasio H, Grabowski TJ. 2002. Normal neuroanatomical variation in the human brain: an MRI-volumetric study. Am J Phys Anthropol 118:341–358.

Andrews TJ, Halpern SD, Purves D. 1997. Correlated size variations in human visual cortex, lateral geniculate nucleus, and optic tract. J Neurosci 17:2859–2868.

Bridge H, Thomas O, Jbabdi S, Cowey A. 2008. Changes in connectivity after visual cortical brain damage underlie altered visual function. Brain 131:1433–1444.

Bridge H, von dem Hagen EAH, Davies G, Chambers C, Gouws A, Hoffmann M, Morland AB. 2012. Changes in brain morphology in albinism reflect reduced visual acuity. Cortex. In press. http://dx.doi.org/10.1016/j.cortex.2012.08.010.

Brodsky MC, Glasier CM, Creel DJ. 1993. Magnetic resonance imaging of the visual pathways in human albinos. J Pediatr Ophthalmol Strabismus 30:382–385.

Bruesch SR, Arey LB. 1942. The number of myelinated and unmyelinated fibers in the optic nerve of vertebrates. J Comp Neurol 77:631–665.

Carroll WM, Jay BS, McDonald WI, Halliday AM. 1980. Two distinct patterns of visual evoked response asymmetry in human albinism. Nature 286:604–606.

Cohen B. 2001. Explaining psychological statistics. New York: John Wiley & Sons.

Creel DJ. 1971. Visual system anomaly associated with albinism in the cat. Nature 231:465–466.

Creel D, Witkop CJ Jr, King RA. 1974. Asymmetric visually evoked potentials in human albinos: evidence for visual system anomalies. Invest Ophthalmol 13:430–440.

Creel D, O'Donnell FE Jr, Witkop CJ Jr. 1978. Visual system anomalies in human ocular albinos. Science 201:931–933.

Devlin JT, Sillery EL, Hall DA, Hobden P, Behrens TE, Nunes RG, Clare S, Matthews PM, Moore DR, Johansen-Berg H. 2006. Reliable identification of the auditory thalamus using multi-modal structural analyses. Neuroimage 30: 1112–1120.

Elschnig A. 1913. Zur Anatomie des menschlichen Albinoauges. Graefes Arch Opthalmol 84:401–419.

Fonda G, Thomas H, Gore GV 3rd. 1971. Educational and vocational placement, and low-vision corrections in albinism. A report based on 253 patients. Sight Sav Rev 41: 29–36.

Fujita N, Tanaka H, Takanashi M, Hirabuki N, Abe K, Yoshimura H, Nakamura H. 2001. Lateral geniculate nucleus: anatomic and functional identification by use of MR imaging. AJNR Am J Neuroradiol 22:1719–1726.

Fulton AB, Albert DM, Craft JL. 1978. Human albinism. Light and electron microscopy study. Arch Ophthalmol 96: 305–310.

Guillery RW. 1986. Neural abnormalities of albinos. Trends Neurosci 9:364–367.

Guillery RW, Kaas JH. 1973. Genetic abnormality of the visual pathways in a "white" tiger. Science 180:1287–1289.

Guillery RW, Casagrande VA, Oberdorfer MD. 1974. Congenitally abnormal vision in Siamese cats. Nature 252:195–199.

Guillery RW, Okoro AN, Witkop CJ Jr. 1975. Abnormal visual pathways in the brain of a human albino. Brain Res 96: 373–377.

Guillery RW, Hickey TL, Kaas JH, Felleman DJ, Debruyn EJ, Sparks DL. 1984. Abnormal central visual pathways in the brain of an albino green monkey (*Cercopithecus aethiops*). J Comp Neurol 226:165–183.

Gupta N, Greenberg G, de Tilly LN, Gray B, Polemidiotis M, Yücel YH. 2009. Atrophy of the lateral geniculate nucleus in human glaucoma detected by magnetic resonance imaging. Br J Ophthalmol 93:56–60.

Hickey TL, Guillery RW. 1979. Variability of laminar patterns in the human lateral geniculate nucleus. J Comp Neurol 183:221–246.

Hoffmann MB, Lorenz B, Morland AB, Schmidtborn LC. 2005. Misrouting of the optic nerves in albinism: estimation of the extent with visual evoked potentials. Invest Ophthalmol Vis Sci 46:3892–3898.

Kastner S, Schneider KA, Wunderlich K. 2006. Beyond a relay nucleus: neuroimaging views on the human LGN. Prog Brain Res 155:125–143.

Klemen J, Hoffmann MB, Chambers CD. 2012. Cortical plasticity in the face of congenitally altered input into V1. Cortex 48:1362–1365.

Kugelman TP, Van Scott EJ. 1961. Tyrosinase activity in melanocytes of human albinos. J Invest Dermatol 37:73–76.

Lund RD. 1965. Uncrossed visual pathways of hooded and albino rats. Science 149:1506–1507.

Malpeli JG, Baker FH. 1975. The representation of the visual field in the lateral geniculate nucleus of *Macaca mulatta*. J Comp Neurol 161:569–594.

Morland AB, Hoffmann MB, Neveu M, Holder GE. 2002. Abnormal visual projection in a human albino studied with functional magnetic resonance imaging and visual evoked potentials. J Neurol Neurosurg Psychiatry 72: 523–526.

Parravano JG, Toledo A, Kucharczyk W. 1993. Dimensions of the optic nerves, chiasm, and tracts: MR quantitative comparison between patients with optic atrophy and normals. J Comput Assist Tomogr 17:688–690.

Rosenberg ML, Jabbari B. 1987. Nystagmus and visual evoked potentials. J Clin Neuroophthalmol 7:133–138.

Rosset A, Spadola L, Ratib O. 2004. OsiriX: an open-source software for navigating in multidimensional DICOM images. J Digit Imaging 17:205–216.

Salinas-Navarro M, Jiménez-López M, Valiente-Soriano FJ, Alarcón-Martínez L, Avilés-Trigueros M, Mayor S, Holmes T, Lund RD, Villegas-Pérez MP, Vidal-Sanz M. 2009. Retinal ganglion cell population in adult albino and pigmented mice: a computerized analysis of the entire population and its spatial distribution. Vision Res 49: 637–647.

Sanderson KJ, Guillery RW, Shackelford RM. 1974. Congenitally abnormal visual pathways in mink (*Mustela vision*) with reduced retinal pigment. J Comp Neurol 154:225–248.

Schmitz B, Schaefer T, Krick CM, Reith W, Backens M, Käsmann-Kellner B. 2003. Configuration of the optic chiasm in humans with albinism as revealed by magnetic resonance imaging. Invest Ophthalmol Vis Sci 44:16–21.

Schneider KA, Richter MC, Kastner S. 2004. Retinotopic organization and functional subdivisions of the human lateral geniculate nucleus: a high-resolution functional magnetic resonance imaging study. J Neurosci 24:8975–8985.

Summers CG. 1996. Vision in albinism. Trans Am Ophthalmol Soc 94:1095–1155.

von dem Hagen EA, Houston GC, Hoffmann MB, Jeffery G, Morland AB. 2005. Retinal abnormalities in human albinism translate into a reduction of grey matter in the occipital cortex. Eur J Neurosci 22:2475–2480.

von dem Hagen EA, Hoffmann MB, Morland AB. 2008. Identifying human albinism: a comparison of VEP and fMRI. Invest Ophthalmol Vis Sci 49:238–249.

Wagner AL, Murtagh FR, Hazlett KS, Arrington JA. 1997. Measurement of the normal optic chiasm on coronal MR images. AJNR Am J Neuroradiol 18:723–726.